



Article

Techno-Economic Feasibility Analysis of an Off-Grid Solar-Wind-Battery Hybrid Renewable Energy System for the Kara Adishuho Community, Northern Ethiopia

Amaha Kidanu Atsbeha^{1,*} and Gebrekiros Gebreyesus Gebremariam²¹ Department of Mechanical Engineering, Raya University, Main Campus, Maichew, P.O. Box 92, Ethiopia² Department of Electrical and Computer Engineering, Raya University, Main Campus, Maichew, P.O. Box 92, Ethiopia

* Correspondence: amahakidanu12@gmail.com or kiros2004comp@gmail.com

How To Cite: Atsbeha, A.K.; Gebremariam, G.G. Techno-Economic Feasibility Analysis of an Off-Grid Solar-Wind-Battery Hybrid Renewable Energy System for the Kara Adishuho Community, Northern Ethiopia. *Renewable and Sustainable Energy Technology* 2026, 2(1), 6. <https://doi.org/10.53941/rset.2026.100003>

Received: 11 October 2025

Revised: 6 February 2026

Accepted: 4 March 2026

Published: 17 March 2026

Abstract: Reliable electricity access remains a major challenge for rural communities in northern Ethiopia, where grid supply is scarce and unstable. This study evaluates the techno-economic feasibility of an off-grid solar-wind hybrid renewable energy system (HRES) with battery storage for the Kara Adishuho community. Local solar resources were assessed using a calibrated Angström-Prescott model, while wind speed data across multiple heights were analyzed with HOMER Pro to optimize system design. The proposed configuration is designed to meet an average daily electricity demand of 1.5 MWh/day, with photovoltaic (PV) panels providing approximately 75% (≈ 1.125 MWh/day), wind turbines contributing 25% (≈ 0.375 MWh/day), and a lithium-ion battery bank supplying short-term backup and operational buffering. Resource assessment indicates an average solar potential of 5.61 kWh/m²/day and a mean wind speed of 2.56 m/s at 10 m, corresponding to a wind power density of approximately 12.46 W/m². Simulation results demonstrate that the hybrid system substantially reduces diesel dependence, achieving estimated annual greenhouse gas savings of ≈ 7.3 tCO₂-eq. Economic evaluation reveals a net present value (NPV) of USD 0.45 million, an internal rate of return (IRR) of 9.5%, and a levelized cost of energy (LCOE) of 0.42 USD/kWh, which is competitive with diesel-based electricity generation in remote areas. These findings confirm that a battery-supported solar-wind hybrid system offers a technically reliable, environmentally sustainable, and economically viable solution for rural electrification, energy resilience, and fossil fuel reduction in northern Ethiopia.

Keywords: resources assessment; renewable energy; solar resource; wind resource; hybrid system

1. Introduction

Access to electricity is a cornerstone of socio-economic development, yet rural electrification remains a persistent challenge in many developing countries, including Ethiopia. Approximately 85% of Ethiopia's population resides in rural areas, but less than 30% have access to reliable electricity [1]. The country's power generation is heavily reliant on hydropower ($\sim 90\%$ of installed capacity), with limited contributions from wind ($\sim 8\%$) and thermal plants. This dependence on hydropower makes the energy sector vulnerable to seasonal rainfall fluctuations, resulting in recurrent power shortages and blackouts. Northern communities, such as Kara Adishuho, face particularly acute electricity access challenges due to limited grid coverage. Driven by climate change concerns and global decarbonization commitments, the renewable energy sector has grown rapidly worldwide, with total installed capacity increasing by 32% from 2023 to 2024, reaching approximately 4448 GW, including



Copyright: © 2026 by the authors. This is an open access article under the terms and conditions of the Creative Commons Attribution (CC BY) license (<https://creativecommons.org/licenses/by/4.0/>).

Publisher's Note: Scilight stays neutral with regard to jurisdictional claims in published maps and institutional affiliations.

1600 GW of photovoltaic (PV) and 1021 GW of wind installations [2]. This global trend underscores the potential of hybrid renewable energy systems (HRES) as reliable and sustainable alternatives to conventional energy production [3–5].

Ethiopia possesses substantial renewable energy potential. The northern highlands, including Kara Adishuho, receive abundant solar radiation (4.5–6.5 kWh/m²/day) and experience favorable wind speeds (5–8 m/s), providing complementary resources for hybrid solar-wind systems. Large-scale projects like the Ashegoda Wind Farm demonstrate the feasibility of harnessing wind energy in the region, while solar PV offers a decentralized option suitable for off-grid communities [6]. Advances in photovoltaic technologies, declining installation costs, and a high solar capacity factor of 4.8 further strengthen the case for hybrid system deployment in rural Ethiopia [7–9]. HRES combining solar PV, wind, batteries, and occasionally diesel backup have been shown to reduce the levelized cost of electricity (LCOE) and improve reliability compared to diesel-only or single-source systems [10–13]. In such configurations, solar PV typically provides the bulk of energy due to high irradiance, while wind complements it intermittently, reducing dependency on batteries or generators [14–16]. Simulation and optimization tools, including HOMER Pro, is essential for system sizing and design, ensuring technical feasibility and cost-effectiveness under local climate and load conditions.

The integration of complementary resources, such as solar, wind, and pumped hydroelectric storage, enhances the reliability of hybrid systems by mitigating the intermittency of individual energy sources [17–20]. Recent studies highlight that dynamic analysis and optimal sizing of PV/Wind-pumped hydro systems are critical for sustainable electricity generation and economic viability in both rural and utility-scale applications [21,22]. Geographical conditions and topography further influence the technical and economic feasibility of hybrid projects, while pumped hydropower storage has been shown to stabilize power delivery, improve system reliability, and reduce long-term operational costs [23–26]. Investigations of standalone PV/Wind-pumped hydro configurations confirm their potential as environmentally friendly, technically feasible, and cost-effective alternatives to conventional energy solutions, particularly in regions with abundant renewable resources [27,28].

Beyond pumped hydro, hybrid systems incorporating diesel and battery storage (PV/Wind/Diesel/Battery microgrids) have proven effective for enhancing rural electrification and off-grid access while reducing reliance on fossil fuels [29,30]. Reviews of microgrid integration emphasize the importance of technical optimization and advanced modeling approaches to maximize reliability and efficiency [31]. Additionally, hybrid systems have demonstrated potential in mitigating power shortages in national grids through economically and environmentally optimized designs [32–34]. Case studies on isolated renewable hybrid systems provide practical insights into system layout, sizing, and operational challenges across diverse contexts [35]. Collectively, these findings indicate that HRES whether pumped hydro-supported, microgrid-based, or grid-connected offer a critical pathway toward resilient, sustainable, and cost-effective energy development.

Despite these global and regional advancements, a notable research gap remains for rural Ethiopian communities. Many existing studies rely on generalized meteorological data and lack comprehensive techno-economic optimization, limiting their applicability to local contexts such as Kara Adishuho. Addressing this gap requires site-specific assessments that integrate measured meteorological data, load profiles, and optimization tools to ensure reliable, cost-effective, and scalable solutions.

This study aims to evaluate the techno-economic feasibility of a solar-wind hybrid system for the Kara Adishuho community. By combining field-collected solar and wind data with HOMER Pro and PVsyst simulations, the research seeks to design an optimized hybrid configuration capable of delivering continuous, affordable, and sustainable electricity. The outcomes are expected to inform rural electrification strategies, support Ethiopia's transition to clean energy, and provide a replicable framework for similar underserved communities across Sub-Saharan Africa.

2. Methodology

The study follows a systematic approach to assess and design the hybrid energy system for Kara Adishuho, structured into distinct phases: resource data gathering, load estimation, system modeling, and techno-economic analysis. The proposed methods encompass a wide variety of generation technologies applicable to both centralized and distributed power systems, while also addressing relevant social and environmental constraints. Data for this research were gathered from both primary and secondary sources to evaluate the viability of a solar PV-wind hybrid system in the Kara Adishuho community. Primary data comprised onsite measurements of solar radiation and wind speed collected through installed sensors, ensuring localized and precise information. Supplementary data were acquired from NASA's database and the National Meteorological Service Agency (NMSA) of Ethiopia. The integration of these diverse datasets facilitated a comprehensive assessment of the energy resource potential, as

illustrated in Figure 1. The study utilized Geographic Information System software (ArcGIS version 10.5, available at <https://www.esri.com/en-us/arcgis> (accessed on 1 September 2025) for managing, analyzing, and visualizing geospatial data. Additionally, HOMER Pro 3.16 (available at <https://www.homerenergy.com> (accessed on 1 December 2025) was employed to model and optimize microgrid configurations, enabling the simulation and evaluation of various system designs. Microsoft Office 365 Excel served as a tool for data organization and detailed analysis. Collectively, these tools formed a robust framework for spatial analysis, microgrid optimization, and data management, significantly contributing to the accuracy and effectiveness of the study.

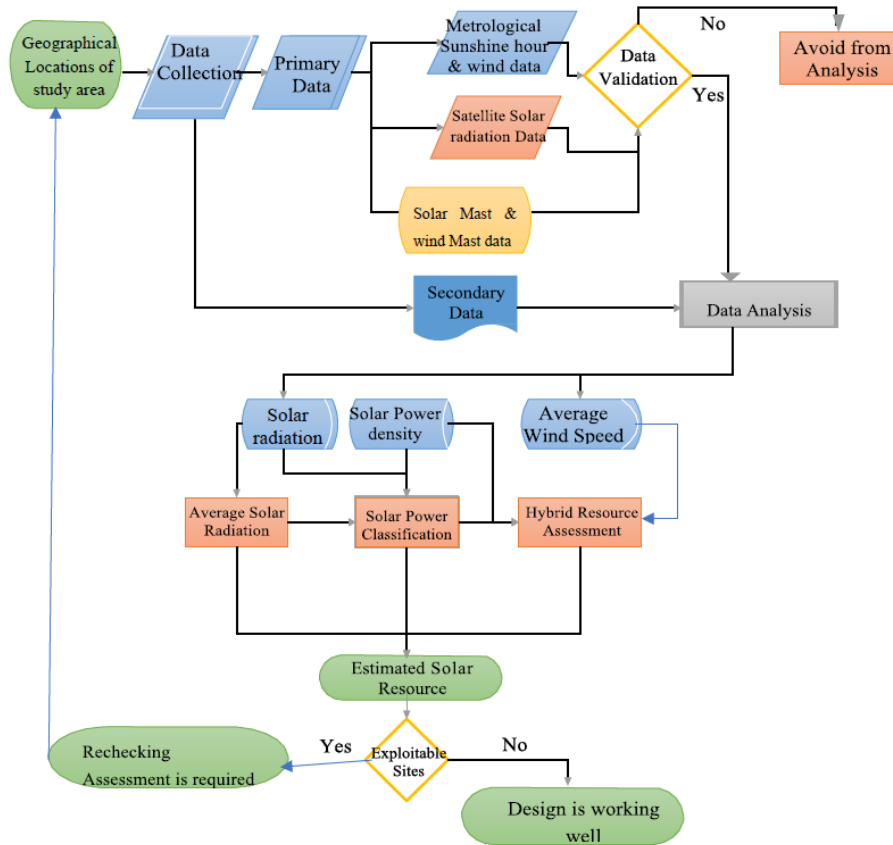


Figure 1. Flow chart of methods and methodology.

2.1. Geographical Locations of Study Area and Data Settings

Ethiopia is geographically positioned within the solar belt, spanning latitudes from 3° to 15° north and longitudes between 33° and 48° east. To assess solar resource potential, a suitability analysis was conducted over the entire Kara Adishuho community area, located in northern Ethiopia. The local temperature at the station varies between 1 °C and 35 °C, with predominantly clear skies for nearly all months throughout the year. The broader Tigray region holds notable energy resource potential due to its location within recognized territorial boundaries. Specifically, Raya Azebo Wereda, and more precisely Kara Adishuho, lies in northern Ethiopia at GPS coordinates ranging from 12°46'27" to 12° 51'8" N latitude and 39°34'6" to 39°55'19" E longitude, as illustrated in Table 1. The Wereda sits at an elevation between 1500 and 2300 m above sea level, experiencing average temperatures between 15 °C and 35 °C. the location of the study area is illustrated in Figure 2.

Table 1. Geographical details of the selected village.

No.	Name of the Village	Description
1	District	Tigray
2	Country	Ethiopia
3	Population	5525
4	Households	921
5	Average family Size	6
6	Longitude	39°38.754' E (39.6459° E)
7	Latitude	12°48.17' N (12.8028° N)
8	Altitude	2479 m (8133 feet) above sea level

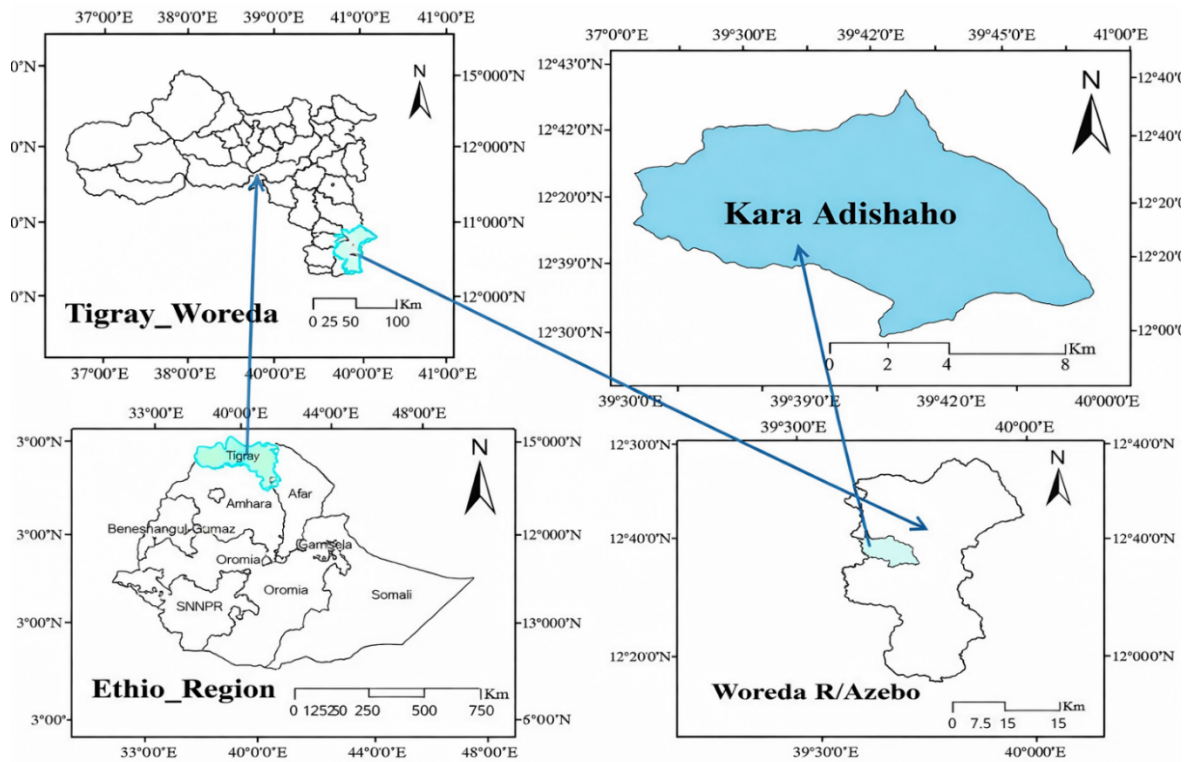


Figure 2. Geographical locations of study area.

2.2. Potential Resource Assessment

For the simulation, both wind and solar energy resources were incorporated in the design of a hybrid renewable energy system. The selected village experiences substantial solar radiation throughout the year. During the summer months, solar insolation is available for approximately 10–12 h per day, whereas in winter, it decreases slightly to around 8–10 h. The maximum ambient temperature at the site during summer reaches 15 °C to 35 °C. Solar radiation data were obtained from the National Aeronautics and Space Administration (NASA) database. For the region under study, the annual average solar radiation and clearness index are 5.71 kWh/m²/day and 0.634, respectively. As illustrated in Figure 2, the monthly solar radiation profile confirms the high potential of the site for solar energy applications and its suitability for electrification through solar-based systems.

2.3. New Estimation Model of Solar Radiation for Kara Adishuho Stations

A modified Angstrom relation was selected for use in the region after reviewing several methods applied in Ethiopia and other countries, based on their suitability for the local conditions. This modified approach offers an improved, topography-dependent model [36,37], that serves as an effective initial input formulas are summarized in Table 2.

Table 2. Numerical formulas and data for solar radiation estimation at Kara Adishuho.

No	Formula/Parameter	Description/Notes
1	$H = H_o \left[a + b \frac{N}{N_o} \right]$	• Classic Angstrom Linear Relation for daily global solar radiation (kWh/m ² /day).
2	$a = -0.309 + 0.539 \cos \phi - 0.0693h + 0.29(N/N_o)$	• Regression coefficient ‘a’, latitude- and topography-dependent.
3	$b = 1.529 - 1.027 \cos \phi + 0.0926h - 0.359(N/N_o)$	• Regression coefficient ‘b’ & latitude.
4	$N_o = \frac{24}{\pi} \times \omega_s = \frac{2}{15} \times \cos^{-1} [-\tan(\phi) \times \tan(\delta)]$	• Maximum possible daylight hours in a day (hours).
5	$\omega_s = \cos^{-1} [-\tan(\phi) \times \tan(\delta)]$	• Sunset hour angle (radians or degrees).
6	$\delta = 23.49^\circ \times \sin \left[360^\circ \times \left(\frac{284 + nd}{365} \right) \right]$	• Solar declination angle (°), n ^d = day of year.
7	$\delta = 0.409 \times \sin \left[\frac{2\pi}{365} \times nd - 1.39 \right]$	• Alternative declination formula (radians).

Table 2. Cont.

No	Formula/Parameter	Description/Notes
8	$H_o = \frac{24}{\pi} \times G_{sc} \times Dr \left[\frac{\pi}{180} \omega_s \times \sin(\varphi) \times \sin(\delta) + \cos(\varphi) \times \cos(\delta) \times \sin(\omega_s) \right]$	• Extraterrestrial daily solar radiation (kWh/m ² /day).
9	$H_o = \frac{24 \times 3600 \times G_{sc}}{\pi} \left[1 + 0.033 \cos\left(\frac{360 \times nd}{365}\right) \right] \times \left[\cos(\varphi) \cos(\delta) \sin(\omega_s) + \frac{\pi \times \omega_s}{180} \sin(\varphi) \sin(\delta) \right]$	• Detailed formula including Earth-Sun distance correction.
11	$G_{on} = G_{sc} \left[1 + 0.033 \cos\left(\frac{360 \times Nd}{365}\right) \right]$	• Extraterrestrial solar radiation on a plane normal to radiation (W/m ²).
12	$E_{PV} = P_{STC} \left[1 + \beta_p(T_{cell} - T_{stc}) \right] \frac{H_t}{H_{stc}}$	• PV module energy output (W), adjusting for irradiance and temperature.
13	$T_{cell} = T_{\infty} + 7.8 \times 10^{-2} H_t$	• Empirical PV cell temperature estimation (°C).

2.4. Wind Energy Resource Potential

Wind resources are as important as solar resources for designing hybrid power systems, and accurate data were obtained from Ethiopian national meteorological stations. Wind speed, caused by air movement from high- to low-pressure areas, is a key meteorological parameter affecting weather forecasting, construction, aviation, maritime activities, and plant growth. The cup anemometer, valued for its simplicity and reliability, measures wind speed by tracking cup rotations, with the anemometer factor (ratio of actual wind speed to shaft speed) typically ranging from 1.5 m/s to 3.0 m/s at 2m height. These measurements, calculated using standard equations, provide essential data for assessing and utilizing wind energy. Wind speed calculations are performed using eqns are summarized in Table 3.

Table 3. Numerical formulas for wind energy and battery storage modeling.

No	Formula	Description
1	$V_{inst} = AF \times \omega$	• Instantaneous wind speed, where AF is the anemometer factor and ω is shaft speed.
2	$V_{avg} = AF \times (N/t)$	• Average wind speed based on number of rotations per unit time.
3	$WPD = 0.5 \times \rho \times V^3$	• Wind power density (W/m ²), where ρ is air density and V is wind speed.
4	$P_{wt} = f(V_z, t)$	• Wind turbine power output as a function of hub-height wind speed and turbine characteristics (cut-in, rated, cut-off).
5	$V_{z,t} = V_{o,t} \left(\frac{h_z}{h_o}\right)^\alpha$	• Wind speed at hub height, where $\alpha = 1/7$ is the wind shear coefficient.
6	Wind energy = $0.5 \times q \times A \times V^3$	• Overall wind energy
7	$SoC_{Dis}(t) = SoC(t - \Delta t)(1 - \sigma) - E_{LV,HV}(t)\eta_b$	• Battery state of charge during discharge mode.
8	$SoC_{ch}(t) = SoC(t - \Delta t)(1 - \sigma) + \left(\frac{P_s(t)}{\eta_{inv}}\right)\eta_b$	• Battery state of charge during charging mode.

2.5. Effective Modeling Software

Several software tools are available for the feasibility assessment of energy generation systems, including HOMER, iHOGA, RETScreen, and Hybrid2 [21]. Each modeling platform offers distinct capabilities in terms of application scope, analytical approach, and power range. In this study, HOMER Pro software was selected due to its widespread adoption, user-friendly interface, and strong capability for off-grid system modeling. In addition, the software enables system sizing based on both technical feasibility and economic viability [22]. HOMER Pro was developed by the National Renewable Energy Laboratory (NREL), USA, specifically for the analysis and optimization of renewable energy systems. The software allows users to define detailed component specifications and evaluates various cost metrics, including life-cycle cost, operation and maintenance cost, net present cost, and levelized cost of energy. In this work, the hybrid system comprises wind turbines, solar photovoltaic (PV) modules, batteries, and power converters of different capacities. HOMER Pro was employed to identify the most feasible system configuration that satisfies the load demand while minimizing overall system cost.

2.6. Electricity Load Assessment

The electrical load demand of the selected village was reasonably estimated based on the existing load profile of a comparable rural village within the same region. In addition, the lifestyle and energy-use preferences of local residents were taken into account. Seasonal variations in electricity demand were evaluated by considering both winter and summer conditions, accounting for differences in appliance usage duration and power ratings typical of rural households. The residential load demand includes common household appliances such as televisions, radios, refrigerators, compact fluorescent lamps (CFLs), and other essential electrical devices widely used in rural communities. The detailed load profile of the selected village is presented in Table 4. The village comprises 335 households, each with an average family size of six members. The estimated average daily electricity consumption is 1505.49 kWh/day in summer, and a peak load demand of 1059.27 kWh/day. The influence of seasonal variations on load demand during winter and summer was incorporated into the analysis to ensure accurate system sizing and performance evaluation.

Table 4. Estimated load demand of the village.

No.	Appliances	Qty	Wattage (W)	Summer		Winter	
				hrs./Day	Wh/Day	hrs./Day	Wh/Day
1	Small refrigerator (fridge)	1	90	24	2160	18	1620
2	CFL lamps (AC)	5	12	7	252	9	324
3	Ceiling fans	3	36	8	864	0	0
4	Water pumps	1	500	1	500	1	500
5	Washing machine	1	500	1	500	1	500
6	Mobile charge	2	8	3	48	3	48
7	Radio Charger	1	10	2	20	2	20
8	TV with receiver	1	50	3	150	3	150
Total energy demand load for 1 household					4494		3162
Total energy demand load for 335 households					1,505,490		1,059,270

3. Details of the Designed Model

The techno-economic evaluation and optimal design of the proposed system require comprehensive technical specifications and cost data for all components involved in the modeling process. In this study, the analysis was carried out using HOMER Pro software, which is widely used for assessing the feasibility and performance of hybrid energy systems. Detailed descriptions of the system components and the overall system configuration are presented in the subsequent sections.

3.1. Details of the System Components

The proposed system for the selected village integrates wind and solar resources as the main sources of renewable energy generation. The system configuration includes wind turbines, photovoltaic (PV) panels, energy storage batteries, and a power converter. The technical specifications and cost-related information for each system component were collected through a comprehensive review of relevant literature and detailed market surveys.

3.1.1. The Wind Turbine Components

A generic wind turbine was selected for the proposed system, and its technical characteristics are summarized in Table 5. The initial investment and replacement costs of the wind turbine were both assumed to be USD 4000, while the annual operation and maintenance cost was estimated at USD 200. Consistent with previous studies, the wind turbines were connected to the AC load [38].

Table 5. Technical parameters of the wind turbine used in the proposed system.

No.	Parameter	Specification
1	Turbine model	Generic with rated capacity 3 kW
2	The Hub height	10 m
3	The Manufacturer	Generic type
4	The Design lifetime	25 years

3.1.2. Battery Energy Storage System

To maintain supply reliability during evening hours and other periods of reduced generation, battery storage was included as a supporting element of the system design. The proposed hybrid configuration employs a 1 kWh lead-acid battery, with detailed technical characteristics summarized in Table 6. For modeling purposes, the upfront investment cost per battery was taken as USD 62, while the replacement cost was assumed to be USD 50. Annual operation and maintenance expenses were estimated at USD 6 per unit, and the battery lifetime was assumed to be five years [39].

$$\text{Figure Battery Capacity} = \frac{\text{Load Demand (MWh)} \times \text{Backup Duration (hours)}}{\text{Depth of Discharge (DoD)} \times \text{Efficiency Factor} \times (1 - \text{loss coefficient})} \quad (1)$$

Table 6. Technical specifications of the storage battery.

No.	Parameter	Specification
1	Storage model	BAE PVS Block
2	The nominal capacity voltage	12 Volts
3	The nominal capacity energy	0.869 kWh
4	The maximum capacity current	72.4 Ah
5	The round-trip system efficiency	85%
6	The maximum capacity charge—discharge current	11.2–119 A respectively

3.1.3. The Solar PV Panels Components

The solar photovoltaic (PV) array was integrated into the DC bus of the proposed hybrid energy system. For modeling purposes, the capital and replacement costs of the PV modules were each assumed to be USD 350 per kW, reflecting current market conditions. Owing to the minimal maintenance needs of PV technology, the annual operation and maintenance cost was set at USD 5 per kW. To represent real-world performance losses arising from factors such as temperature variation, dust accumulation, and wiring inefficiencies, a derating factor of 88% was applied to the PV modules [25]. The complete technical parameters of the PV system are summarized in Table 7.

Table 7. Technical specifications of the solar PV panels.

No.	Parameter	Description
1	Module model	CS6K-290MS (All-Black series)
2	PV technology	Flat-plate photovoltaic module
3	Nominal power rating	1 kW
4	Manufacturer	Canadian Solar Inc.
5	Expected operational lifetime	25 years

3.1.4. The Converter Components

An ideal power converter with a rated capacity of 30 kW (model 30B3-4DF) was incorporated into the system to facilitate AC–DC power conversion. For simulation purposes, both the initial investment cost and the replacement cost were taken as USD 104 per kW, while the operational lifetime of the converter was assumed to be 15 years as illustrated in Table 8. The conversion efficiency of the inverter stage was set at 96%, consistent with typical performance values reported in the literature [26]. The complete technical specifications of the converter are summarized in Table 9.

Table 8. Technical characteristics of the power converter.

No.	Converter Specification	
1	Maximum power rating	30 kW
2	Rated current capacity	39A
3	Operating voltage range	480 VACS to 400 VACS
4	Operating frequency	60Hz or 50Hz
5	Nominal—Peak conversion efficiency	96–97% respectively
7	Expected service lifetime	15 years

Table 9. Overall cost breakdown of the system.

No.	System Component	Initial Investment Cost (\$)	Replacement Cost (\$)	Annual Operating Cost (\$)
1	Wind turbine	4000.00 \$	4000.00 \$	200.00 \$
2	Solar PV modules	350.00 \$	350.00 \$	5.00 \$
3	Power converter	104.00 \$	104.00 \$	0.00 \$
4	Battery storage	62.00 \$	50.00 \$	6.00 \$

3.2. The Hybrid System Model Configuration

The hybrid renewable energy system combines wind, solar, battery storage, and a power converter to supply reliable electricity to a rural community. PV modules, batteries, and the converter connect to the DC bus, while the wind turbine feeds the AC load. Excess energy charges the batteries, ensuring continuous supply during low-generation periods. System optimization in HOMER Pro considered technical and economic metrics, showing the chosen configuration achieves the lowest NPC, COE, and O&M costs, with illustrating component cost contributions.

$$\text{Figure Battery Capacity} = \frac{\text{Load Demand (MWh)} \times \text{Backup Duration (hours)}}{\text{Depth of Discharge (DoD)} \times \text{Efficiency Factor} \times (1 - \text{loss coefficient})} \quad (2)$$

Photovoltaic (PV) panels typically achieve efficiencies of 15% to 22% and have a lifespan of 25 to 30 years, with performance influenced by factors such as temperature and shading [40,41]. Wind turbines vary in rated power, often exceeding 2 MW, with capacity factors of 30% to 50% depending on local wind conditions. They are generally mounted at heights between 80 and 120 m, which enhances energy capture [42]. For sizing optimization in hybrid renewable energy systems, the primary objective is to minimize the Levelized Cost of Energy (LCOE) while maximizing energy output. Constraints include technical limits on power output, financial budgets, and environmental regulations, alongside reliability concerns like Loss of Power Supply Probability. The Levelized Cost of Energy (LCOE) and the payback time money (PBTM). The cost of environmental damage produced by carbon dioxide (C_{CO_2}) may be used to compute LCOH using the following Equation [43]:

$$\text{LCOE} = \frac{\left(\frac{r(1+r)^n}{(1+r)^n - 1} \right) \times C + C_{O\&M} - C_{CO_2}}{E_t} \quad (3)$$

$$\text{PBTM} = \frac{C}{\frac{(1+r)^n - 1}{r(1+r)^n} (C_{CO_2} - C_{O\&M})} \quad (4)$$

The cost of environmental damage (C_{CO_2}) caused by CO_2 gas can be calculated by the following Equation [44].

$$C_{CO_2} = EF_{CO_2} \times E_t \times \phi_{CO_2} \quad (5)$$

where: EF_{CO_2} represents the CO_2 emission factor of the electric power generation system (kg CO_2 /kWh) [45], ϕ_{CO_2} represents the carbon social cost (\$/ton CO_2), which may be considered as \$70/ton CO_2 [46].

The environmental and social impacts of PV solar fields are well addressed in Assessment of Environmental and Social Impacts of Photovoltaic Solar Fields [47]. The study highlights both the ecological considerations, such as land use and habitat alteration, and the social benefits, including job creation and improved local energy access.

3.3. Economic Analysis

The economic viability of the proposed hybrid renewable energy system was assessed using key financial indicators, including the net present cost (NPC), cost of energy (COE), initial capital investment, and operation and maintenance (O&M) expenses. These metrics provide a comprehensive evaluation of both the short-term and long-term financial performance of the system. The analysis helps determine the most cost-effective configuration while ensuring reliable energy supply throughout the year.

3.4. System Constraints and Uncertainty Analysis

The isolated HRES is designed to supply the Governorate’s load independently, with reliability evaluated via the PSROC [48]. Key uncertainties arise from PV module characteristics (irradiance, temperature, technology), conversion chain losses (inverter/transformer efficiency, MPPT, module mismatch, design/workmanship), and

long-term degradation, collectively defining the overall uncertainty in predicted energy yield, which will be quantified at the end of the section.

$$\text{The total uncertainties} = \sqrt{\sum(\text{individual uncertainty})^2} \tag{6}$$

4. Results and Discussion

The assessment of renewable resource potential in Kara Adishuho was carried out through the application of a modified Angstrom model for solar radiation estimation, coupled with measured wind data extrapolated to turbine hub height. The results were integrated into a hybrid PV-wind-battery energy system simulation using HOMER Pro, and subsequently analyzed in terms of energy potential, techno-economic performance, and environmental implications.

4.1. Solar Energy Resource Potential

The modified Angstrom relation was applied to the sunshine duration data collected from Raya Azebo Wereda, producing the monthly average daily global solar radiation values. Solar radiation, as detailed in Section 2.1 and summarized in Figure 3, exhibits a distinct seasonal pattern. The site receives a high annual average of 5.61 kWh/m²/day, with peak insolation of 6.5 kWh/m²/day in November during the dry season. The minimum radiation of 4.1 kWh/m²/day occurs in August, coinciding with the rainy season and increased cloud cover. This variation underscores the need for a complementary energy source or robust storage to ensure supply continuity during periods of low solar availability.

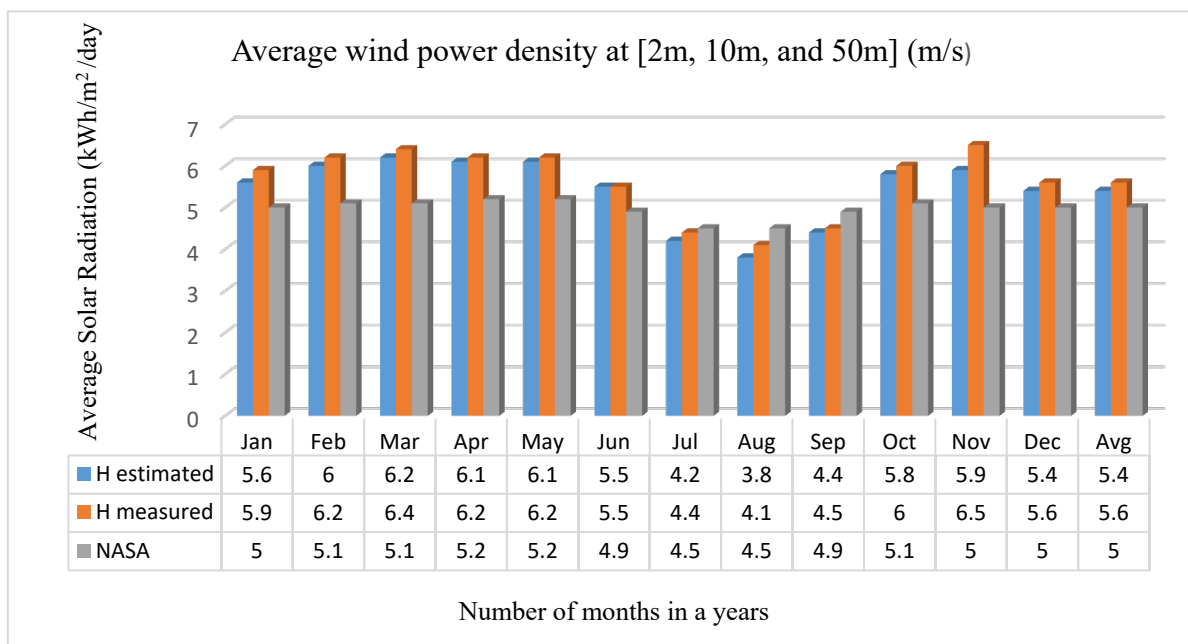


Figure 3. Monthly average solar radiation data.

4.2. Wind Energy Resource Potential

Measured wind speeds at 2 m, 10 m, and 50 m were extrapolated to an 80 m hub height using the wind shear law with an exponent of 1/7, yielding an average speed of 2.73 m/s and a corresponding wind power density of 12.46 W/m². While this limits the feasibility of utility-scale projects, small-scale turbines could still contribute to energy diversification. Interestingly, the wind resource exhibits an inverse correlation with solar availability (Figure 4), with monthly average wind speeds peaking in March and July and dropping to their lowest in September and October across all measured heights. Power density follows this pattern, reaching maxima of 10.55 W/m² at 2 m, 19.85 W/m² at 10 m, and 37.34 W/m² at 50 m, with 10 m identified as the most practical design height, balancing infrastructure feasibility and energy yield as shown in Figure 5. To further characterize the resource, the Rayleigh probability distribution was applied to model wind speed frequency, estimating equivalent power densities between 150–200 W/m² at 10 m height. For an 80 m² swept area and air density of 1.225 kg/m³, the potential wind power at the observed 2.73 m/s average speed.

$$\text{Wind energy} = 0.5 \times \rho \times A \times V^3 \tag{7}$$

$$\text{Wind energy} = 0.5 \times 1.225 \text{ kg/m}^3 \times 80 \text{ m}^2 \times (19.85 \text{ m/s})^3 = 375205 \text{ Wh/day} = 375 \text{ kWh/day}$$

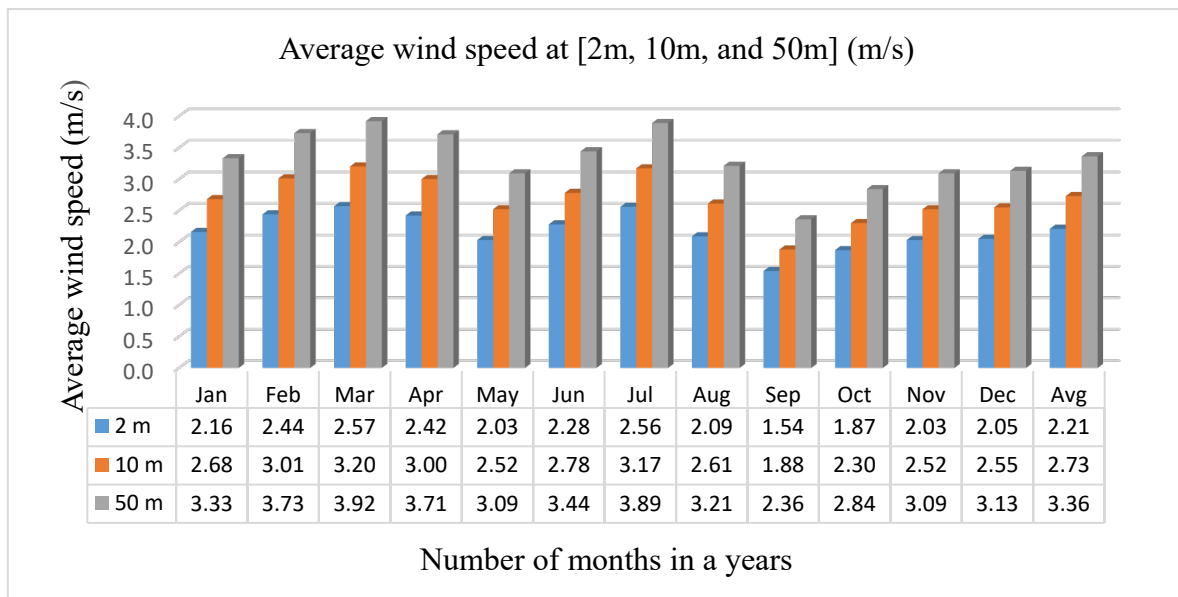


Figure 4. Monthly average wind Speed.

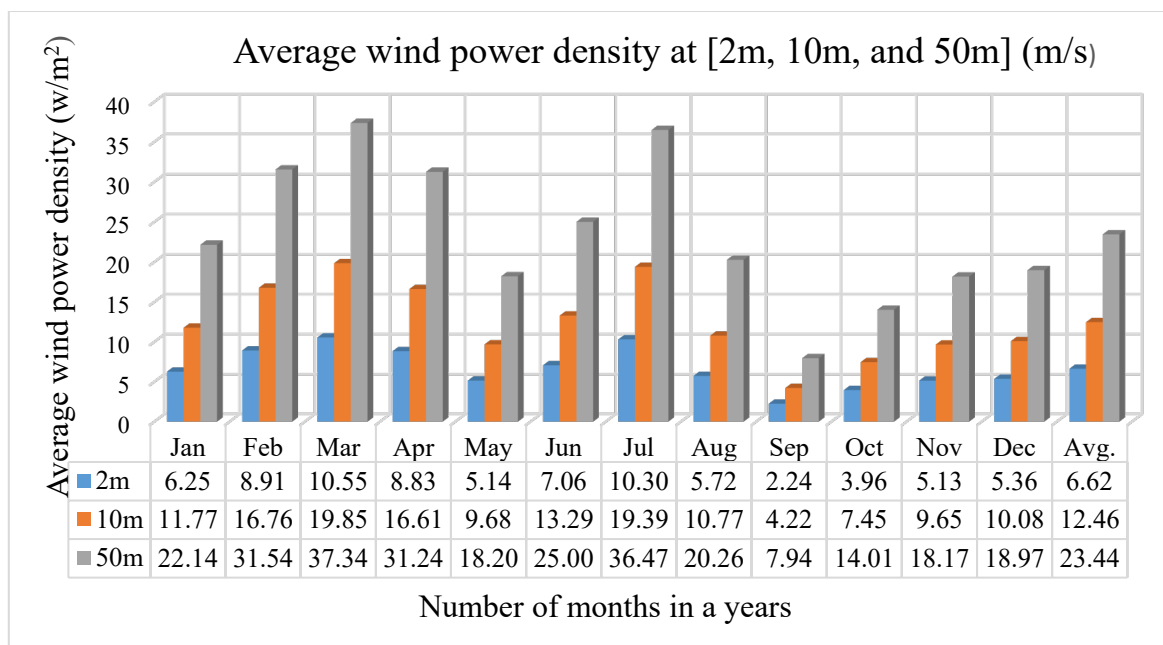


Figure 5. Monthly average wind power density.

4.3. Solar-Wind Hybrid Energy Generation

The hybrid solar-wind system combines PV panels and wind turbines to exploit their complementary output. The design process includes site assessment, energy modeling, component sizing, integration, storage planning, and economic analysis, aiming to generate 1.5 MWh/day (75% solar, 25% wind). PV and wind components are selected to meet energy targets, while battery storage mitigates variability. Simulations consider local irradiance, wind, and storage needs, ensuring component compatibility and cost-effectiveness. This integrated system improves reliability and efficiency compared to standalone sources, as shown in Figure 6.

A lithium-ion battery bank with a nominal capacity of 40 kWh was assumed to evaluate system storage. Considering an inverter efficiency of 90%, a round-trip battery efficiency of 85%, and a depth of discharge of 80%, the effective usable storage capacity is approximately 24.5 kWh. This level of storage provides short-term backup (several hours) for the hybrid system and primarily supports evening and night-time demand smoothing,

rather than multi-day autonomy. For a cluster of 335 households with an average daily electricity consumption of 1.2–1.5 kWh per household, the total community demand ranges from 402 to 503 kWh/day, indicating that the battery system functions as an operational buffer rather than a standalone energy supply. Consequently, the battery bank plays a critical role in enhancing power reliability during periods of reduced solar irradiance and low wind availability.

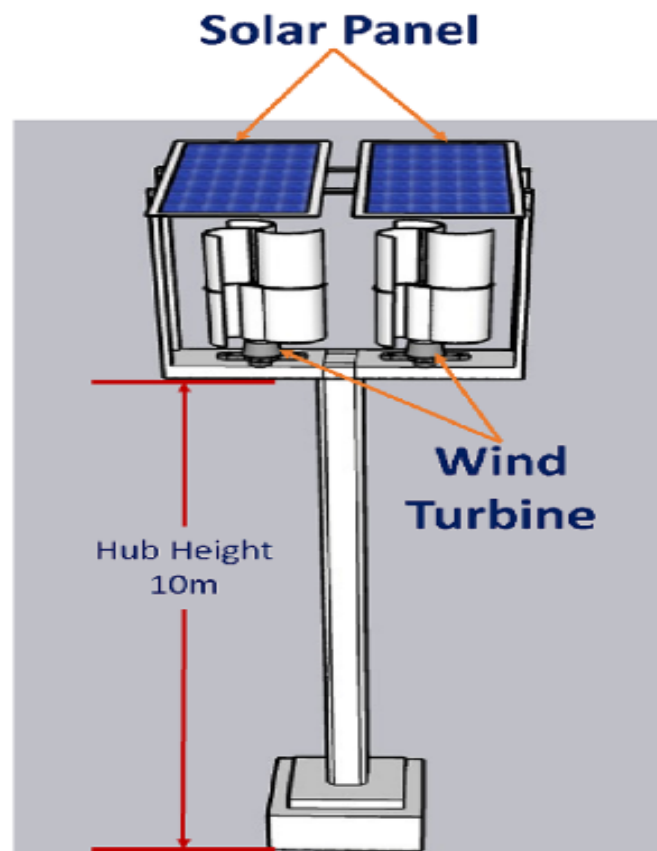


Figure 6. Schematic diagram of solar PV-wind hybrid power supply system.

Uncertainties in resource measurement and system performance were also evaluated. Solar radiation data variability contributed $\pm 5\%$, PV module efficiency $\pm 3\%$, inverter and battery efficiencies $\pm 2\%$, and wind speed measurements $\pm 10\%$. Applying a root-sum-square method, the combined uncertainty was estimated to be approximately $\pm 12\%$. This level of uncertainty is acceptable for rural electrification feasibility studies and does not significantly affect the overall conclusion that solar PV is the dominant energy resource for the Kara Adishuho hybrid renewable energy system.

4.4. Technology Assessment Methodology

Before finalizing the hybrid configuration, a comprehensive evaluation of technology performance, reliability, and environmental compatibility under local conditions was conducted, as illustrated in Figure 7. Technology selection is pivotal in renewable energy projects, as it directly influences cost-effectiveness, operational reliability, and long-term sustainability. For the photovoltaic (PV) subsystem, the EVO 6 N panel was selected due to its high conversion efficiency of 22.5%, low degradation rate, and long operational lifespan. Based on system sizing and resource availability, the PV array was designed to generate approximately 1.125 MWh/day, accounting for nearly 75% of the total daily energy demand. To complement solar generation, the wind subsystem was designed to supply the remaining 25% of demand, corresponding to approximately 0.375 MWh/day. A Savonius vertical-axis wind turbine (VAWT) was selected owing to its robustness under low and turbulent wind regimes, mechanical simplicity, and extended service life of approximately 25 years. While Savonius turbines exhibit lower aerodynamic efficiency than horizontal-axis turbines, their reliability and suitability for the local wind conditions justify their inclusion as a supplementary energy source.

Battery energy storage underpins system reliability by mitigating the variability between renewable generation and load demand. A lithium-ion battery bank was adopted due to its high round-trip efficiency ($\approx 90\%$),

allowable depth of discharge ($\approx 80\%$), and low degradation characteristics. Rather than serving as full energy storage for daily demand, the battery system was sized to provide short-term autonomy and operational buffering, supporting evening and night-time loads and enhancing system stability during periods of reduced solar or wind generation. The storage capacity was therefore optimized for reliability and cost-effectiveness, rather than full 24-h energy independence. To validate the techno-economic feasibility of the proposed configuration, simulations were carried out in HOMER Pro. HOMER Pro was employed for system optimization, identifying the least-cost combination of PV, wind, and storage components while ensuring technical reliability and minimizing Net Present Cost (NPC). PVsyst provided detailed modeling of the PV subsystem, enhancing the accuracy of generation forecasts and complementing HOMER Pro results. Together, these tools ensured a robust design capable of meeting local demand with both economic and environmental benefits.

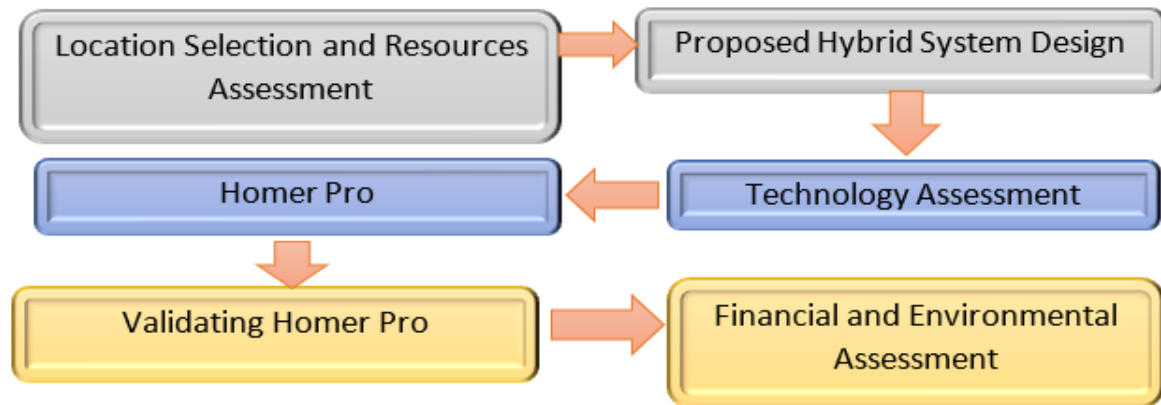


Figure 7. Techno-economics of PV-wind hybrid system flowchart.

The average temperature distribution of the location is illustrated in Figure 8, as shown below. The clearness index, shown in Figure 9, represents the fraction of solar radiation reaching the Earth’s surface relative to the extraterrestrial (top-of-atmosphere) solar radiation and exhibits pronounced seasonal variation at the study site. The highest clearness index value of 0.749 occurs in November, coinciding with the maximum average daily solar radiation of 6.5 kWh/m²/day, whereas the lowest value of 0.391 is observed in August, corresponding to the minimum solar radiation of 4.1 kWh/m²/day. These results indicate that November is characterized by the clearest atmospheric conditions and highest solar availability, while August experiences increased cloud cover and atmospheric attenuation. Overall, both the clearness index and daily solar radiation reach their peak values during late autumn and winter and decline during the summer months, highlighting the strong seasonal influence on solar energy potential at the site.

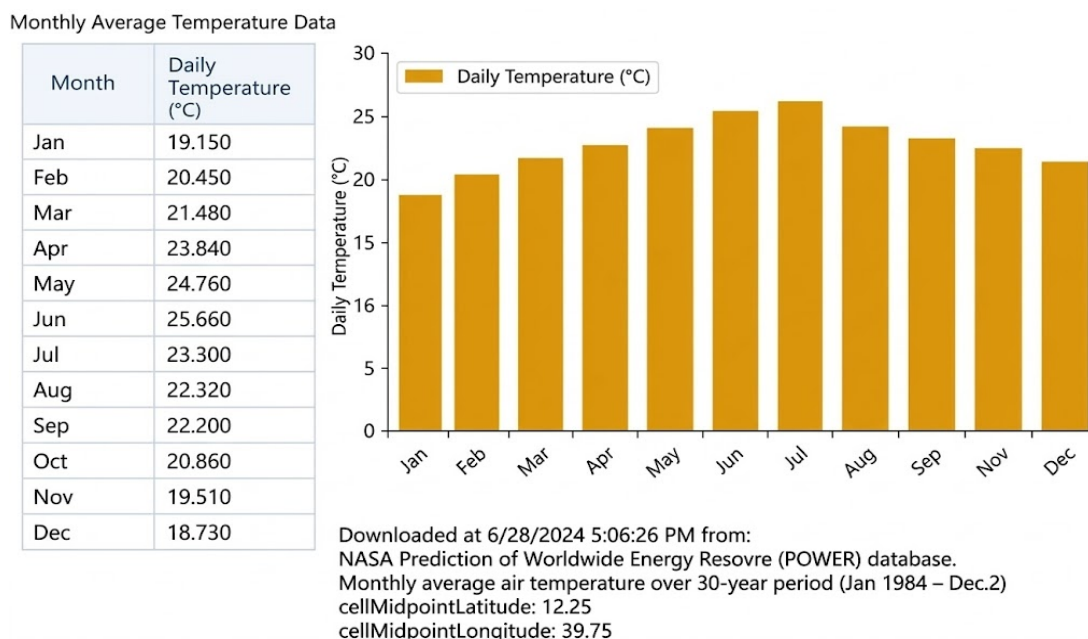


Figure 8. Demand with both economic and environmental benefits.

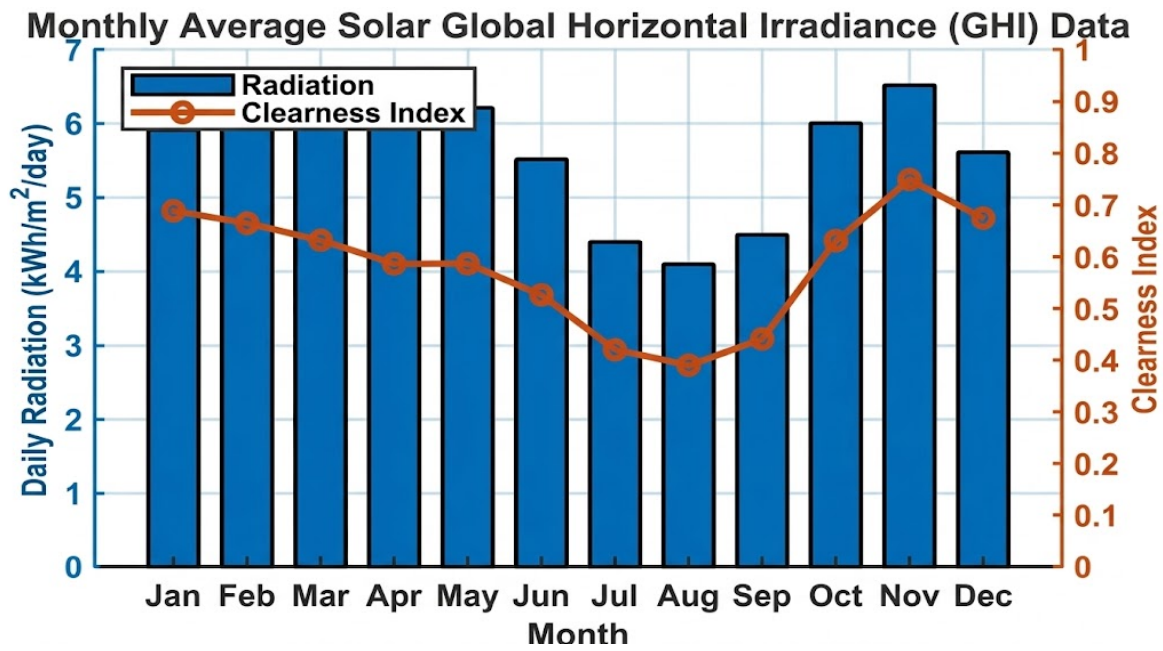


Figure 9. Monthly average global horizontal irradiance (GHI) for Kara Adishuho site.

Wind speeds also display a clear seasonal pattern, with the highest velocities recorded in late winter and early spring. The maximum average monthly wind speed of 19.85 m/s occurs in March, as shown in Figure 10, while the minimum value of 4.22 m/s is observed in September. A secondary peak of 19.39 m/s is recorded in July. The substantial variation of 15.63 m/s between peak and low wind periods indicates strong seasonal fluctuations in wind activity, likely influenced by regional and large-scale atmospheric circulation patterns. These trends highlight the importance of accounting for seasonal wind variability when designing and optimizing renewable energy systems for the study site.

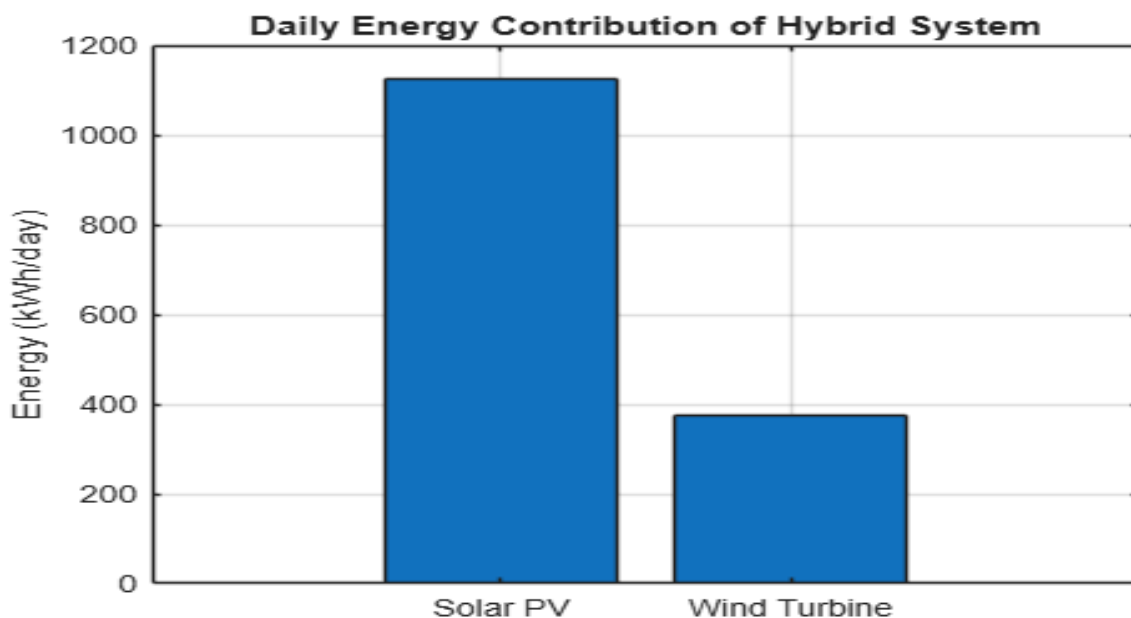


Figure 10. Daily energy contribution of solar PV and wind turbine in the hybrid system.

4.4.1. The Optimization Results

HOMER Pro simulation software conducts thousands of iterations to determine the most feasible and optimal hybrid system configuration by varying the capacities of solar PV, wind, and battery components. Each feasible configuration is evaluated and ranked according to its net present cost (NPC), with the lowest NPC indicating the most cost-effective option. The optimal hybrid system, which achieves the minimum NPC, is summarized in Table 10.

Table 10. Optimization results of the hybrid energy system.

	Architecture					Costs			System	
	Solar PV (kW)	Wind Turbine	Battery	Converter (kW)	Dispatch	NPC (\$)	COE (\$)	O&M (\$)	Initial Capital (\$)	Renewable Fraction (%)
1	103	4	224	29.1	CC	127,345	0.137	4522	68,882	100
2	120		355	30	CC	140,048	0.15	5640	67,132	100

The simulation results indicate that the hybrid system comprising solar PV, wind turbines, and battery storage represents the most optimized configuration. The optimal setup consists of 103 kW of solar PV capacity, four wind turbines each rated at 3 kW, 224 lead-acid batteries (12 V, 72.4 Ah each), and a 29.1 kW power converter. This configuration achieves the lowest cost of energy (COE) of \$0.137/kWh compared to the other system combinations evaluated.

The chart shows that the hybrid system’s daily energy production is dominated by solar PV, contributing approximately 1125 kWh/day, while wind turbines supply about 375 kWh/day. This reflects the system’s design strategy of relying primarily on solar energy, with wind serving as a complementary source to meet total demand as shown in Figure 10. Based on the data, the installed capacity of the Solar PV system is 235 kW. In comparison, the installed Wind Turbine system has a smaller capacity of 45 kW as shown in Figure 11.

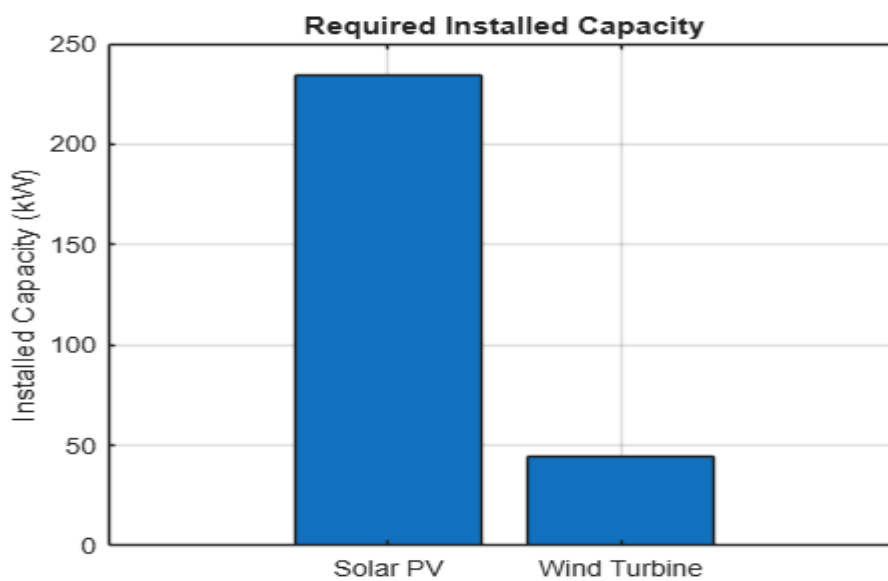


Figure 11. Comparison of installed renewable energy capacity.

4.4.2. System Economic Analysis

The financial evaluation of the solar photovoltaic (PV)-wind hybrid system in Kara Adishuho is based on an average electricity generation of approximately 1.5 MWh/day, comprising 1.125 MWh/day from solar PV and 0.375 MWh/day from wind energy, corresponding to an annual energy production of 547.5 MWh. The total initial capital investment is estimated at approximately USD 1.7 million, covering the costs of solar PV arrays, wind turbines, hybrid inverters, battery storage, and associated balance-of-system infrastructure. Annual operational and maintenance (O&M) costs, including routine maintenance and system management, are projected at approximately USD 55,000. Assuming an electricity tariff of USD 0.12/kWh, annual electricity sales are estimated at approximately USD 65,700. In addition, avoided diesel fuel consumption contributes estimated savings of USD 50,000 per year, resulting in total annual benefits of approximately USD 115,700. Based on these combined revenues and cost savings, the simple payback period of the project is estimated to be approximately 14.7 years.

The cost assessment incorporates capital expenditure, operation and maintenance costs, and long-term project economics. Capital costs are distributed across system components, including solar PV modules, wind turbines, battery storage, inverters, and balance-of-system components. Using a capital recovery factor (CRF) of 0.102 and assuming annual O&M costs equivalent to 2% of the initial capital investment, the annualized system cost is estimated at approximately USD 228,000 per year. Dividing this value by the annual electricity generation of 547.5 MWh yields a levelized cost of energy (LCOE) of approximately USD 0.42/kWh as expressed in Figure 12. While

this value exceeds Ethiopia's grid electricity tariff (below USD 0.10/kWh), it remains competitive with the cost of diesel-based electricity generation, typically ranging from USD 0.45 to 0.70/kWh in remote areas.

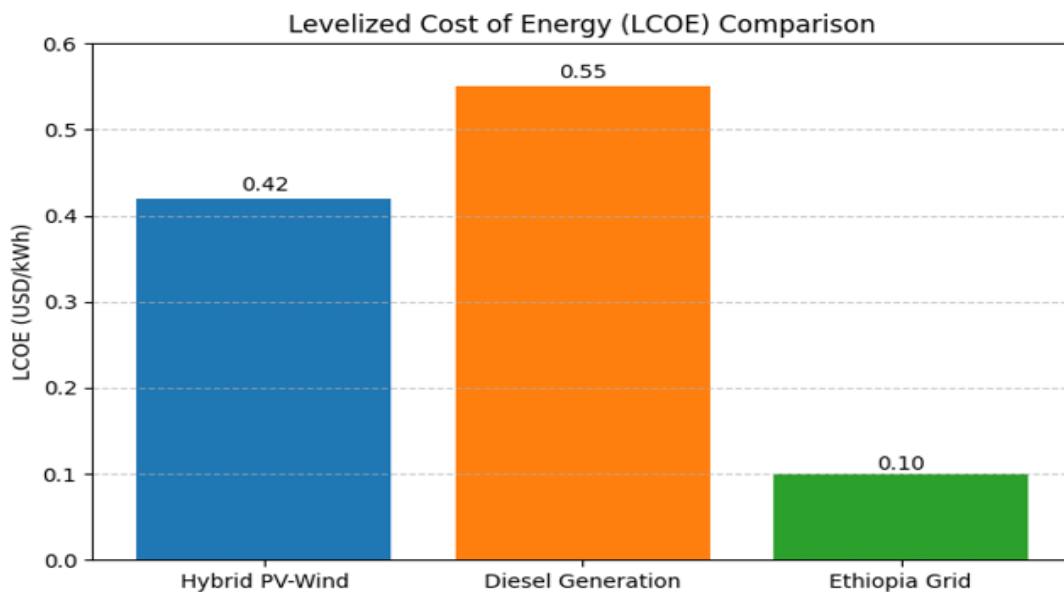


Figure 12. Levelized cost of energy (LCOE) comparison by source.

From an environmental perspective, the hybrid renewable energy system displaces an estimated 7.3 tons of CO₂ emissions annually, corresponding to environmental benefits valued at approximately USD 511 per year based on prevailing carbon pricing assumptions. Over a projected project lifetime of 20 years, the net present value (NPV) is estimated at approximately USD 450,000, with an internal rate of return (IRR) of 9.5%, indicating favorable long-term financial performance. Sensitivity analyses further confirm the robustness of the project's economic viability under variations in capital cost, fuel savings, and electricity tariffs. Overall, the proposed hybrid PV-wind system represents a financially viable, technically reliable, and environmentally sustainable solution for providing dependable electricity to the Kara Adishuho community and serves as a replicable model for rural electrification in similar contexts. Consistent with previously published studies [49,50], the proposed approach demonstrates greater feasibility in terms of both economic efficiency and user comfort.

5. Conclusions and Future Work

Despite the inherent variability of wind and solar energy resources, their complementary characteristics play a crucial role in optimizing energy generation, improving power stability, and enhancing the reliability of hybrid wind-photovoltaic systems. The analysis conducted at hourly, diurnal (day–night), and monthly (seasonal) time scales demonstrates that solar and wind resources at the study site exhibit sufficiently complementary availability patterns. In particular, an inverse relationship between solar radiation and wind speed is observed, which is advantageous for balancing power generation within the hybrid system.

The site's average annual solar irradiation was estimated at approximately 2130 kWh/m², corresponding to a daily average of 5.84 kWh/m²/day. The minimum observed daily solar radiation of 4.1 kWh/m²/day provides a conservative reference for photovoltaic (PV) system sizing and reliability assessment. Wind resource analysis indicates relatively low but usable wind speeds. The average wind speed at the site is approximately 2.56 m/s, yielding a mean wind power density of about 12.46 W/m². Solar radiation, with peak instantaneous values ranging from approximately 1030 to 1556 W/m² and average daytime power densities between 390 and 650 W/m², effectively complements the wind resource and reinforces the dominance of solar PV in the hybrid configuration. Based on these resource characteristics, the optimized hybrid renewable energy system (HRES) was designed to meet an average daily electricity demand of 1.5 MWh, with photovoltaic generation supplying approximately 75% of the total energy demand and wind energy contributing the remaining 25%. Battery energy storage was incorporated to provide short-term autonomy and operational buffering, ensuring system reliability during periods of reduced renewable generation and minimizing reliance on diesel backup generation.

The deployment of the optimized hybrid system significantly reduces diesel fuel consumption, resulting in an estimated annual reduction of ≈7.3 tCO₂-eq. Economically, the system demonstrates robust performance, with a net present value (NPV) of USD 0.45 million and an internal rate of return (IRR) of 9.5% over a 20-year project

lifetime. The levelized cost of energy (LCOE) remains competitive with diesel-based electricity in remote areas, providing a sustainable and economically viable solution for rural electrification. Using a capital recovery factor (CRF) of 0.102 and assuming annual operation and maintenance (O&M) costs equivalent to 2% of the initial capital investment, the annualized system cost is approximately USD 228,000. Dividing this by the annual electricity production of 547.5 MWh yields an LCOE of ~USD 0.42/kWh, which, although higher than Ethiopia's grid tariff (<USD 0.10/kWh), is lower than the typical diesel generation cost of USD 0.45–0.70/kWh in remote regions.

For future research, it is recommended to apply advanced modeling techniques and remote sensing technologies to further refine solar and wind resource assessments across Ethiopia. In addition, expanded analyses of socio-economic impacts and regional comparisons would provide valuable insights for energy policy and planning. Ongoing work aims to deliver a comprehensive assessment of solar PV-wind hybrid potential in northern Ethiopia, supporting sustainable electricity generation and enhancing energy resilience in the Kara Adishuho community.

Author Contributions

A.K.A.: conceptualization, methodology, writing, original draft preparation, writing, reviewing and editing, visualization; G.G.G.: data curation, conceptualization, reviewing and editing, investigation, editing, supervision. All authors have read and agreed to the published version of the manuscript.

Funding

This research received no external funding.

Institutional Review Board Statement

The study was conducted according to the guidelines of the Declaration of Helsinki, and approved by the Institutional Review Board (or Ethics Committee).

Informed Consent Statement

Not applicable.

Data Availability Statement

The original contributions presented in this study are included in the article. Further inquiries can be directed to the corresponding author.

Conflicts of Interest

The authors declare no conflict of interest.

Use of AI and AI-Assisted Technologies

During the preparation of this work, the authors used ChatGPT and Grammarly to rephrase sentences and enhance language. After using these tools/services, the authors reviewed and edited the content as needed and take full responsibility for the content of the published article.

Abbreviations

Acronyms	Full Name
PV	Photovoltaic
GIS	Geographic Information Systems
NMSA	National Meteorological Service Agency
CSP	Concentrated Solar Power
NASA	National Aeronautics & Space Administration
IRENA	International Renewable Energy Agency
EPCO	Ethiopian Electricity Power Corporation
GPS	Geographical Position System
HPGS	Hybrid Power Generation System
CSA	Central Statistical Agencies
a \$ b	Constant Coefficients
MAST	Measured Data
PVsyst	Geographical Position System
HRES	Hybrid Renewable Energy Systems

References

1. Hailu, A.D. Ethiopia Hydropower Development and Nile Basin Hydro Politics. *AIMS Energy* **2022**, *10*, 87–101. <https://doi.org/10.3934/ENERGY.2022006>.
2. Nassar, Y.F.; El-Khozondar, H.J.; Fakher, M.A. The Role of Hybrid Renewable Energy Systems in Covering Power Shortages in Public Electricity Grid: An Economic, Environmental and Technical Optimization Analysis. *J. Energy Storage* **2025**, *108*, 115224. <https://doi.org/10.1016/j.est.2024.115224>.
3. Cozzi, L.; Gould, T.; Bouckart, S.; et al. World Energy Outlook 2020. *Energy* **2020**, *2019*, 30.
4. Canton, H. International Energy Agency—IEA. In *The Europa Directory of International Organizations 2021*, 23rd ed.; Routledge: London, UK, 2021; p. 3. <https://doi.org/10.4324/9781003179900-103>.
5. Matragi, I.; Maiboom, A.; Tauzia, X.; et al. Energy Conversion and Management: X A Novel Algorithm for Optimizing Genset Operations to Minimize Fuel Consumption in Remote Diesel-RES Microgrids. *Energy Convers. Manag. X* **2024**, *24*, 100728. <https://doi.org/10.1016/j.ecmx.2024.100728>.
6. Mahmud, A.M.; Kahsay, M.B.; Hailesilassie, A.; et al. Solar Energy Resource Assessment of the Geba Catchment, Northern Ethiopia. *Energy Procedia* **2014**, *57*, 1266–1274. <https://doi.org/10.1016/j.egypro.2014.10.116>.
7. Girma, M.; Assefa, A.; Molinas, M. Feasibility Study of a Solar Photovoltaic Water Pumping System for Rural Ethiopia. *AIMS Environ. Sci.* **2015**, *2*, 697–717. <https://doi.org/10.3934/environsci.2015.3.697>.
8. Selby, J.; Royston, S.; Cox, E. *The Impacts of Non-Energy Policies on the Energy System October 2016 Executive Summary*; UK Energy Research Centre: London, UK, 2016.
9. Sajid, M.U.; Bicer, Y. Comparative Life Cycle Cost Analysis of Various Solar Energy-Based Integrated Systems for Self-Sufficient Greenhouses. *Sustain. Prod. Consum.* **2021**, *27*, 141–156. <https://doi.org/10.1016/j.spc.2020.10.025>.
10. Girma, M.; Molina, M.; Assefa, A. Feasibility Study of a Wind Powered Water Pumping System for Rural. *AIMS Energy* **2015**, *3*, 851–868. <https://doi.org/10.3934/energy.2015.4.851>.
11. Kodicherla, S.P.K.; Gaddada, S.; Shaik, N. Wind Energy Potential and Economic Evaluation of WPS Using WECSs in Three Selected Locations of Northern Ethiopia. *Afr. J. Sci. Technol. Innov. Dev.* **2017**, *9*, 179–187. <https://doi.org/10.1080/20421338.2017.1303990>.
12. Alsop, A.; Eales, A.; Strachan, S.; et al. A Global Market Assessment Methodology for Small Wind in the Developing World. In Proceedings of the 2017 IEEE Global Humanitarian Technology Conference (GHTC), San Jose, CA, USA, 19–22 October 2017. <https://doi.org/10.1109/GHTC.2017.8239226>.
13. Tesfahunegn, W.; Datiko, D.; Wale, M.; et al. Impact of Wind Energy Development on Birds and Bats: The Case of Adama Wind Farm, Central Ethiopia. *J. Basic Appl. Zool.* **2020**, *81*, 41. <https://doi.org/10.1186/s41936-020-00171-1>.
14. Zegeye, A.D. Wind Resource Assessment and Wind Farm Modeling in Mossobo-Harena Area, North Ethiopia. *Wind. Eng.* **2021**, *45*, 648–666. <https://doi.org/10.1177/0309524X20925409>.
15. Teffera, B.; Assefa, B.; Björklund, A.; et al. Life Cycle Assessment of Wind Farms in Ethiopia. *Int. J. Life Cycle Assess.* **2021**, *26*, 76–96. <https://doi.org/10.1007/s11367-020-01834-5>.
16. Gebresslassie, M.G. Development and Manufacturing of Solar and Wind Energy Technologies in Ethiopia: Challenges and Policy Implications. *Renew. Energy* **2021**, *168*, 107–118. <https://doi.org/10.1016/j.renene.2020.11.042>.
17. Abiodun, A.; Paul, O.; Benson, O.; et al. Dynamic Impact of Hybrid Wind-Solar Photovoltaic Power Injection on Small Signal Stability of Nigerian 11kV Power System Using Self Organizing Map Neural Network. *Sci. Afr.* **2024**, *24*, e02214. <https://doi.org/10.1016/j.sciaf.2024.e02214>.
18. Hung, H.; Kang, H.; Lee, A.H.I. Strategic Selection of Suitable Projects for Hybrid Solar-Wind Power Generation Systems. *Renew. Sustain. Energy Rev.* **2010**, *14*, 413–421. <https://doi.org/10.1016/j.rser.2009.08.004>.
19. Ermolenko, B.V.; Ermolenko, G.V.; Fetisova, Y.A.; et al. Wind and Solar PV Technical Potentials: Measurement Methodology and Assessments for Russia. *Energy* **2017**, *137*, 1001–1012. <https://doi.org/10.1016/j.energy.2017.02.050>.
20. Salim, E.; Abubaker, A.; Ahmed, B.; et al. A Brief Overview of Hybrid Renewable Energy Systems and Analysis of Integration of Isolated Hybrid PV Solar System with Pumped Hydropower Storage for Brack City—Libya. *Wadi Alshatti Univ. J. Pure Appl. Sci.* **2025**, *3*, 152–167. https://doi.org/10.63318/waujpasv3i1_22.
21. Muchiri, K.; Ngugi, J.; Wafula, D.; et al. Wind and Solar Resource Complementarity and Its Viability in Wind/PV Hybrid Energy Systems in Machakos, Kenya. *Sci. Afr.* **2023**, *20*, e01599. <https://doi.org/10.1016/j.sciaf.2023.e01599>.
22. Alharthi, Y.Z.; Siddiki, M.K.; Chaudhry, G.M. Resource Assessment and Techno-Economic Analysis of a Grid-Connected Solar PV-Wind Hybrid System for Different Locations in Saudi Arabia. *Sustainability* **2018**, *10*, 3690. <https://doi.org/10.3390/su10103690>.
23. Abass, W.; Somlal, J.; Kumar, S.; et al. Results in Engineering Design and Analysis of a Solar-Wind Hybrid Renewable Energy Tree. *Results Eng.* **2023**, *17*, 100958. <https://doi.org/10.1016/j.rineng.2023.100958>.
24. Khare, V.; Nema, S.; Baredar, P. Solar-Wind Hybrid Renewable Energy System: A Review. *Renew. Sustain. Energy Rev.* **2016**, *58*, 23–33. <https://doi.org/10.1016/j.rser.2015.12.223>.

25. Khan, Z.A.; Imran, M.; Altamimi, A.; et al. Assessment of Wind and Solar Hybrid Energy for Agricultural Applications in Sudan. *Energies* **2022**, *15*, 5. <https://doi.org/10.3390/en15010005>.
26. Bekelea, G.; Boneya, G. Design of a Photovoltaic-Wind Hybrid Power Generation System for Ethiopian Remote Area. *Energy Procedia* **2012**, *14*, 1760–1765. <https://doi.org/10.1016/j.egypro.2011.12.1164>.
27. Hassan, Q.; Algburi, S.; Zuhair, A.; et al. Results in Engineering Review Article A Review of Hybrid Renewable Energy Systems: Solar and Wind-Powered Solutions: Challenges, Opportunities, and Policy Implications. *Results Eng.* **2023**, *20*, 101621. <https://doi.org/10.1016/j.rineng.2023.101621>.
28. Kumar, D.; Tewary, T. Investigating the Sustainability of Urban Energy Generation with Techno-Economic Analysis from Hybrid Energy Systems. *Energy Strategy Rev.* **2023**, *50*, 101250. <https://doi.org/10.1016/j.esr.2023.101250>.
29. Saadat, Z.; Farazmand, M.; Sameti, M. Integration of Underground Green Hydrogen Storage in Hybrid Energy Generation. *Fuel* **2024**, *371*, 131899. <https://doi.org/10.1016/j.fuel.2024.131899>.
30. Cabos, W.; Nieto-borge, C.; Guti, C. Complementarity of Offshore Energy Resources on the Spanish Coasts: Wind, Wave, and Photovoltaic Energy. *Renew. Energy* **2024**, *224*, 120213. <https://doi.org/10.1016/j.renene.2024.120213>.
31. Hu, Z.; Su, R.; Veerasamy, V.; et al. Resilient Frequency Regulation for Microgrids under Phasor Measurement Unit Faults and Communication Intermittency. *IEEE Trans. Ind. Inform.* **2024**, *21*, 1941–1949. <https://doi.org/10.1109/TII.2024.3495785>.
32. KarthickNarayanan, M.; Manoj, K.; Laxmi Narayanan, R.; et al. Virtual Brokerage. *Int. Res. J. Adv. Eng. Hub* **2024**, *2*, 349–354. <https://doi.org/10.47392/irjaeh.2024.0052>.
33. De Oliveira, M.S.; Steffen, V.; Trojan, F. Systematic Literature Review on Electric Vehicles and Multicriteria Decision Making: Trends, Rankings, and Future Perspectives. *J. Intell. Manag. Decis.* **2024**, *3*, 22–41. <https://doi.org/10.56578/jimd030103>.
34. Li, X.; Hu, C.; Luo, S.; et al. Distributed Hybrid-Triggered Observer-Based Secondary Control of Multi-Bus DC Microgrids over Directed Networks. *IEEE Trans. Circuits Syst. I Regul. Pap.* **2025**, *72*, 2467–2480. <https://doi.org/10.1109/TCSI.2024.3523339>.
35. Aqila, A.; Nassar, Y.; El-Khozondar, H.; et al. Design of Hybrid Renewable Energy System (PV/Wind/Battery) Under Real Climatic and Operational Conditions to Meet Full Load of the Residential Sector: A Case Study of a House in Samno Village—Southern Region of Libya. *Wadi Alshatti Univ. J. Pure Appl. Sci.* **2025**, *3*, 168–181. https://doi.org/10.63318/waujpasv3i1_23.
36. Atsbeha, A.K.; Gebremariam, G.G.; Gebru, K.G. Assessment of Solar Resource Potential and Estimation of Direct and Diffuse Solar Irradiation from Sunshine Hours Data for Eastern Zone of Tigray, Northern Ethiopia. *Sustain. Energy Res.* **2025**, *12*, 16. <https://doi.org/10.1186/s40807-025-00162-2>.
37. Atsbeha, A.K.; Gebremariam, G.G.; Gebressie, T.H. Analysis of Sunshine Hours Data and Estimation of Global Solar Radiation for Mychew Tabia Smret Station, Northern. *Sustain. Energy Res.* **2024**, *11*, 38. <https://doi.org/10.1186/s40807-024-00130-2>.
38. Ahmed, J.; Harijan, K.; Shaikh, P.H.; et al. Techno-Economic Feasibility Analysis of an Off-Grid Hybrid Renewable Energy System for Rural Electrification. *J. Electr. Electron. Eng.* **2021**, *9*, 7–15. <https://doi.org/10.11648/j.jee.20210901.12>.
39. Bayu, E.S.; Khan, B.; Hagos, I.G.; et al. Feasibility Analysis and Development of Stand-Alone Hybrid Power Generation System for Remote Areas: A Case Study of Ethiopian Rural Area. *Wind* **2022**, *2*, 68–86. <https://doi.org/10.3390/wind2010005>.
40. Atsbeha, A.K.; Berhe, T.A.; Gebru, M.T. Modelling and Analysis of Flat Plate Solar Air Collector with Phase Change Materials for Extended Surface, Drying Application. *Discov. Energy* **2026**, *6*, 4
41. Ahmad, S.; Agrira, A.; Nassar, Y. The Impact of Loss of Power Supply Probability on Design and Performance of Wind/Pumped Hydropower Energy Storage Hybrid System. *Wadi Alshatti Univ. J. Pure Appl. Sci.* **2025**, *3*, 52–62. https://doi.org/10.63318/waujpasv3i2_06.
42. Elnaggar, M.; El-Khozondar, H.J.; Salah, W.A.; et al. Assessing the Techno-Enviro-Economic Viability of Wind Farms to Address Electricity Shortages and Foster Sustainability in Palestine. *Results Eng.* **2024**, *24*, 103111. <https://doi.org/10.1016/j.rineng.2024.103111>.
43. Elmariami, A.; El-Osta, W.; Nassar, Y.; et al. Life Cycle Assessment of 20 MW Wind Farm in Libya. *Appl. Sol. Energy* **2023**, *59*, 64–78. <https://doi.org/10.3103/S0003701X22601557>.
44. Abdunnabi, M.; Etiab, N.; Nassar, Y.F.; et al. Energy Savings Strategy for the Residential Sector in Libya and Its Impacts on the Global Environment and the Nation Economy. *Adv. Build. Energy Res.* **2023**, *17*, 379–411. <https://doi.org/10.1080/17512549.2023.2209094>.
45. Makhzom, A.M.; Aissa, K.R.; Alshanokie, A.A.; et al. Carbon Dioxide Life Cycle Assessment of the Energy Industry Sector in Libya: A Case Study. *Int. J. Electr. Eng. Sustain.* **2023**, *1*, 145–163. <https://doi.org/10.65998/ijees.v1i3.58>.
46. Eteriki, M.A.; El-Osta, W.A.; Nassar, Y.F.; et al. Effect of Implementation of Energy Efficiency in Residential Sector in Libya. In Proceedings of the 2023 8th International Engineering Conference on Renewable Energy & Sustainability (ieCRES), Gaza, Palestine, 8–9 May 2023; pp. 1–6. <https://doi.org/10.1109/ieCRES57315.2023.10209521>.

47. Al-Maghalseh, M. The Environmental Impact and Societal Conditions of PV Power Plants: A Case Study of Jericho Gate-Palestine Stat Of. *Wadi Alshatti Univ. J. Pure Appl. Sci.* **2025**, 3, 16–31. https://doi.org/10.63318/waujpasv3i2_03.
48. Nassar, Y.F.; Alsadi, S.Y.; El-Khozondar, H.J.; et al. Design of an Isolated Renewable Hybrid Energy System: A Case Study. *Mater. Renew. Sustain. Energy* **2022**, 11, 225–240. <https://doi.org/10.1007/s40243-022-00216-1>.
49. Wastewater, U.; Pryce, D.; Alsharrah, F.; et al. Comparative Life-Cycle Cost Analysis of Alternative Technologies for the Removal of Emerging Contaminants from Urban Wastewater. *Water* **2022**, 14, 1919. <https://doi.org/10.3390/w14121919>.
50. *Active Electrical Distribution Network: A Smart Approach*; John Wiley & Sons: Hoboken, NJ, USA, 2021. ISBN 9781119599517.